Hybrid PMMA–silica anticorrosive coatings for stainless steel 316L

J. L. Varela Caselis*[1], E. Rubio Rosas[1] and V. M. Castaño Meneses[2]

316L stainless steel in environments with high chlorine content suffers localised corrosion. In this study, hybrid sol–gel based anticorrosive protective coatings were developed and deposited on 316L stainless steel substrates. The effect of incorporating different compositions of silica in polymethylmethacrylate (PMMA) sol–gel coatings on the aqueous corrosion resistance of 316L stainless steel in 5 wt-% aqueous NaCl electrolyte was evaluated. Analysis shows that the coatings are uniform, crack free and well bonded to the substrate. Organic–inorganic phases exhibited good compatibility. In addition, the adhesion strength of PMMA–silica hybrid coatings to the surface was found to be higher than the pure system PMMA coating. The anticorrosive properties were evaluated by electrochemical noise and visual test according to ASTM D610 (rusting degree) and ASTM D714 (blistering degree). Coatings with 75 wt-%PMMA–25 wt-% silica possessed the best corrosion performance among the coating specimens.

Keywords: Hybrid coatings, Anticorrosive coatings, Sol–gel coatings, PMMA–silica hybrids

Introduction

316L stainless steel is a corrosion resistant material with respect to other alloys, but in environments with high chloride content, it suffers localised corrosion. Stainless steels are, in general, widely used in industrial, structural, marine, medical and other everyday applications because of their physical characteristics such as strength and comparatively good corrosion resistance compared with other commercial alloys.[1,2] The chromium oxide passivation layer formed on the surface of stainless steel in oxidising environments is the main reason for its corrosion resistance and durability.[3] However, when using stainless steel in an environment containing chloride species, localised corrosion will often occur in the form of pitting.[4,5] For example, AISI 316L stainless steel is regarded as a biocompatible material and has been used in the fabrication of prosthetic devises. However, this alloy may suffer from localised corrosion, releasing significant quantities of dissolved species to neighbouring tissues, leading to the risk of local tumours and mechanical failure of the implant.[6,7]

In order to improve corrosion resistance, the most commonly used strategy to reduce the release of ions is through surface modification methods, including nitriding,[8] surface passivation[9] and electrochemical polishing.[10] However, in practice, the formed film is susceptible to develop pinholes, which may give rise to rapid film degradation under corrosive conditions.[1,3] Therefore, the application of coatings may be necessary to increase the overall corrosion resistance of the alloy.

In recent years, hybrid films sol–gel have attracted a lot of interest due to their outstanding properties, i.e. elastic stiffness, excellent barrier resistance, flame retardant properties, scratch/wear resistance, optical characteristics and electrical and anticorrosive properties.[11–13] Hybrid organic–inorganic materials that have been used to protect metal from corrosion are composed of intimately mixed polymer systems,[14,15] so as to combine the properties of the organics and ceramic materials. The inorganic component tends to impart durability, scratch resistance and improved adhesion to the metal substrates, while the organic components contribute increased flexibility and density. An advantage of hybrid sol–gel systems is the possibility to prepare thick, crack free coatings[16] and of adding particles and/or tailor the presence of specific organic groups.[17] In this regard, the presence of inorganic material may reduce the porosity in the coating, providing a high barrier for the diffusion of aggressive species from the electrolyte to the metal substrate.[14] There are various papers in the literature concerning improving the corrosion resistance of coatings using hybrid systems on metals.[18–20]

Silicon dioxide is one of the most promising ceramics employed in anticorrosion coatings.[21–23] SiO_2 reveals excellent properties such as high strength, excellent wear resistance, high hardness and excellent chemical resistance. It has been demonstrated that hybrid coatings obtained from tetraethylorthosilicate (TEOS) via acidic catalysts improve the corrosion behaviour of stainless steel in environments containing chloride,[24] because the films that are formed are highly adherent and chemically

[1]Centro Universitario de Vinculación, Benemérita Universidad Autónoma de Puebla, Puebla, Mexico
[2]Centro de Física Aplicada y Tecnología Avanzada, Universidad Nacional Autónoma de México, Juriquilla, Querétaro, México.

*Corresponding author, email jvarela11@yahoo.com.mx

Published by Maney on behalf of the Institute
Received 27 May 2011; accepted 14 November 2011
DOI 10.1179/1743278211Y.0000000035

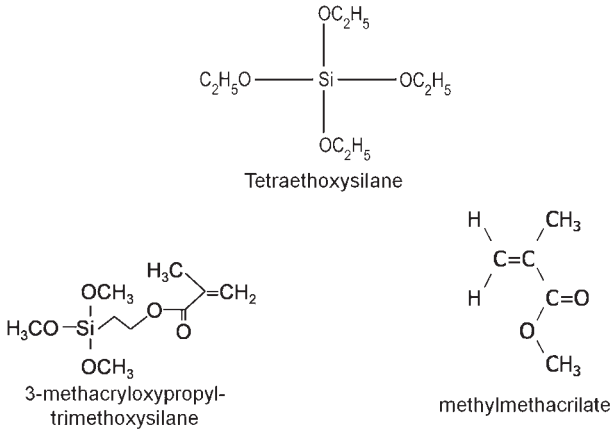

1 Polymethylmethacrylate–silica hybrid system precursors

inert at close to room temperature. Thus, polymethylmethacrylate (PMMA)–silica coatings produced by sol–gel methods provide adequate protective coatings combining anticorrosive properties while maintaining high optical transparency, which allows them to be used as protective aesthetic coatings.

Although the preparation of hybrid PMMA–silica coatings is well studied,[25] there are few reports in the literature related to the corrosion resistance of PMMA–silica hybrid coatings applied to 316L stainless steel. In the present work, the potential of sol–gel PMMA–silica hybrid coatings to improve the adhesion and corrosion performance of 316L stainless steel products in 5% NaCl solution was studied. To ensure appropriate compatibility, nanoscale coatings were prepared with enhanced chemical bonding between the silica network and a PMMA matrix using 3-methacryloxypropyl-trimethoxysilane (TMS) as coupling agent. The synthesised coatings were characterised using scanning electron microscopy (SEM). Fourier transform infrared spectroscopy and an adhesion test (ASTM D3359-02). The effect of different relative concentrations of PMMA–silica on the corrosion performance of the resultant hybrid coatings was investigated using electrochemical noise (EN).

Experimental

Materials

The organic and inorganic phase precursors of the hybrid were methylmethacrylate (MMA) and TEOS respectively. As coupling agent, TMS was employed (Fig. 1). Ethanol (EtOH) was used as solvent with hydrochloric acid as catalyst. All the precursors were purchased from Sigma-Aldrich. As substrates, 316L stainless steel coupons (3×3 cm) were used.

Substrate preparation

The 316L coupons (3×3 cm) were washed and cleaned with detergent and then immersed briefly in nitric acid (HNO_3) to passivate the surface. In order to ensure good adhesion between the substrate surface and the sol–gel hybrid coating, the substrates were etched at elevated temperature for 30 min in persulphuric acid, prepared by reacting 30% hydrogen peroxide (H_2O_2) with concentrate sulfuric acid (H_2SO_4) at 90°C. After etching, the samples were subject to a final rinse in deionised water.

Synthesis of PMMA–silica hybrid

Sol–gel hybrid PMMA–silica coatings were prepared with different molar ratios (Table 1), as follows: TEOS was prehydrolysed by the acidic catalyst of the mixture TEOS/TMS/MMA/H_2O/EtOH (molar ratio: 1 : 0·8 : 4 : 4 respectively) at room temperature for 24 h. The prehydrolysed sol was mixed with benzyl peroxide at 1 mol.-% to an initiator and prepolymerised at 70°C for 30 min. The dip coating method was used to apply the coatings to the stainless steel coupons at a withdrawal rate of 10 cm min^{-1}. The coated 316L coupons were dried at room temperature for 5 min and cured at 70°C for 24 h.

Scanning electron microscopy was performed using a JEOL SEM (model JSM-6610LV) equipped with an Oxford Instruments X-ray energy dispersive analyser. For the Fourier transform infrared spectroscopy, a Bruker spectrometer model Vertex 70 was used, operated in the interval of 500–4000 cm^{-1}.

Pull-off adhesion testing

The adhesive strength pure PMMA polymer and PMMA–silica hybrid sol–gel coatings were evaluated on metallic substrate according to ASTM D 3359-02 (tape pulloff test). The typical procedure is as follows: first, the surface of the sample coated was cut by a razor to make intersecting grid lines. The total test area was ~ 1 cm^2 with each square grid dimension of 1×1 mm. An adhesive tape of 25 mm width, manufactured by Permacel, was applied firmly to cover the grid area of the coating at room temperature. After ~ 90 s, the Permacel tape was stripped off with one quick pull. The adhesion strength of the coatings can be estimated by counting the number of squares peeled off as compared to the original number of squares.

Electrochemical studies

Samples were immersed in 5 wt-% NaCl solution at room temperature and removed for evaluation after 250, 500, 750, 1000, 1250, 1500, 1750, 2000, 2250, 2500, 2750 and 3000 h exposure. The panels were visually inspected according to ASTM D610 (rusting degree) and ASTM D714 (blistering degree), after which EN analysis was carried out. The EN is a very useful technique for the study of organic coatings.[26–28] EN measurements were undertaken using a three-electrode system. The working electrodes (WE_1 and WE_2) were identically coated samples with an exposure area of 1 cm^2. A saturated calomel electrode (SCE) was used as the reference electrode. The electrolyte was 5 wt-% NaCl at room temperature. The EN measurements were carried out with an electrochemical unit (Gill AC from ACM Instruments) coupled to a personal computer, which was used to store data for further analysis; the potential

Table 1 Specification of coatings PMMA–silica hybrid

Sample code	Composition		Dry film thickness/μm
	MMA/mol.-%	TEOS/mol.-%	
100–00	100	0	10
90–10	90	10	9
75–25	75	25	8
50–50	50	50	5
25–75	25	75	2·5
10–90	10	90	0·3

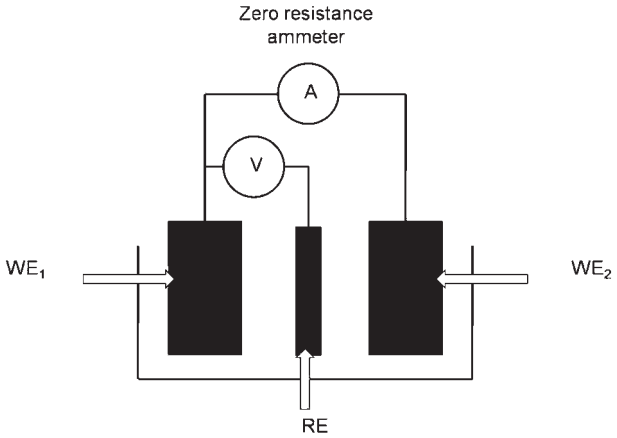

2 Experimental arrangement cell

and current noise data were acquired simultaneously. The method consisted of measuring, as a function of time, the electrochemical potential noise between the working electrode and the saturated calomel referenced electrode, and the electrochemical current noise between the two working electrodes. In the electrochemical potential noise measurements, the specimen was left at the open circuit potential (free corrosion potential). The electrochemical current noise was obtained at the corrosion potential in the three-electrode cell at a sample rate of one reading every second, as establish by Hladky and Dawson.[29,30] After gathering the data as a potential/current time record (time series) of 1024 readings, the dc drift was removed by subtracting a linear regression line from the data.[31]

If both potential and current noises are measured, the standard deviation of potential can be divided by the standard deviation of current to obtain a value with units of resistance, known as the EN resistance R_n. For noise resistance measurements, the experimental arrangement shown in Fig. 2 was employed, using a coupled pair of working electrodes to measure the current noise, with the potential of this coupled pair being measured against a stable reference electrode.

Results and discussion

Figure 3 shows images of the hybrid coating surface at different compositions. The hybrid coatings 100–00, 90–10, 75–25 and 50–50 appear uniform and free of cracks, while coatings 25–75 and 10–90 (Fig. 3*e* and *f*) show cracks and defects. Figure 4 shows cross-sections of the coated 316L coupons, where the coatings are shown to be well bonded and free of defects such as surface blisters or cracks. However, Fig. 4*f* shows that coating 10–90 has internal porous structure. The coating thickness measure on steel samples was between 0·3 and 10 μm.

Figure 5 shows the Fourier transform infrared spectra for PMMA, 3-methacryloxypropyl-trimethoxysilane and hybrid coatings. The characteristic absorption bands of the PMMA appearing at 1436 and 1384 cm^{-1} were

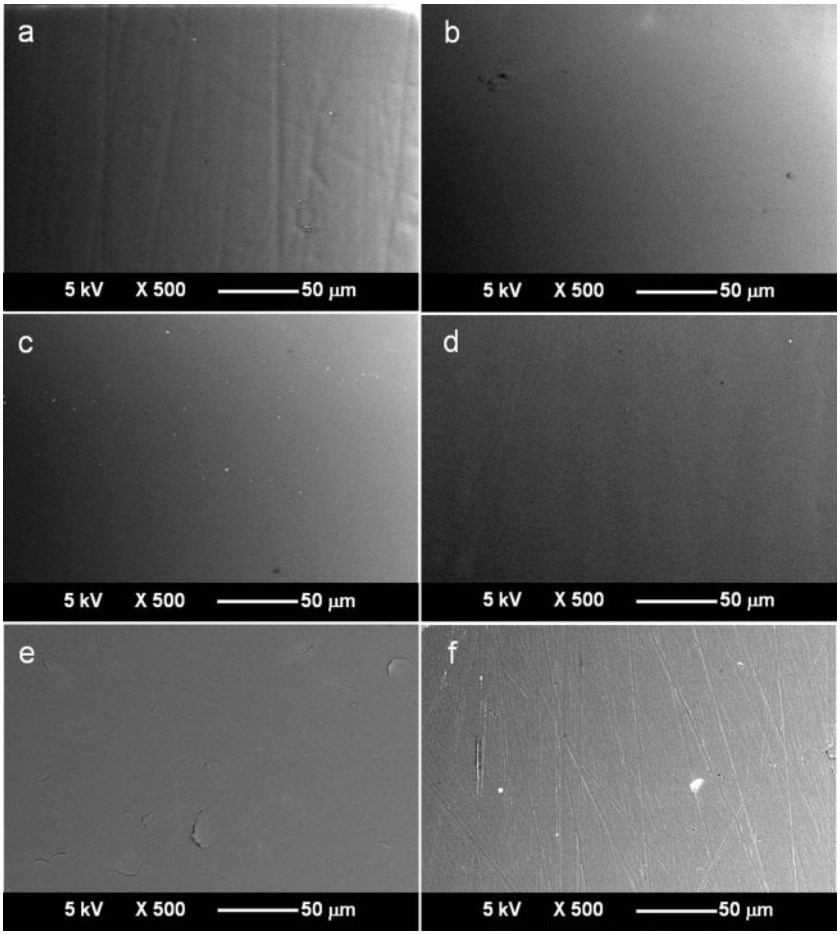

a 100–00; *b* 90–10; *c* 75–25; *d* 50–50; *e* 25–75; *f* 10–90

3 Micrographs of PMMA–silica hybrid coatings to different relative concentrations

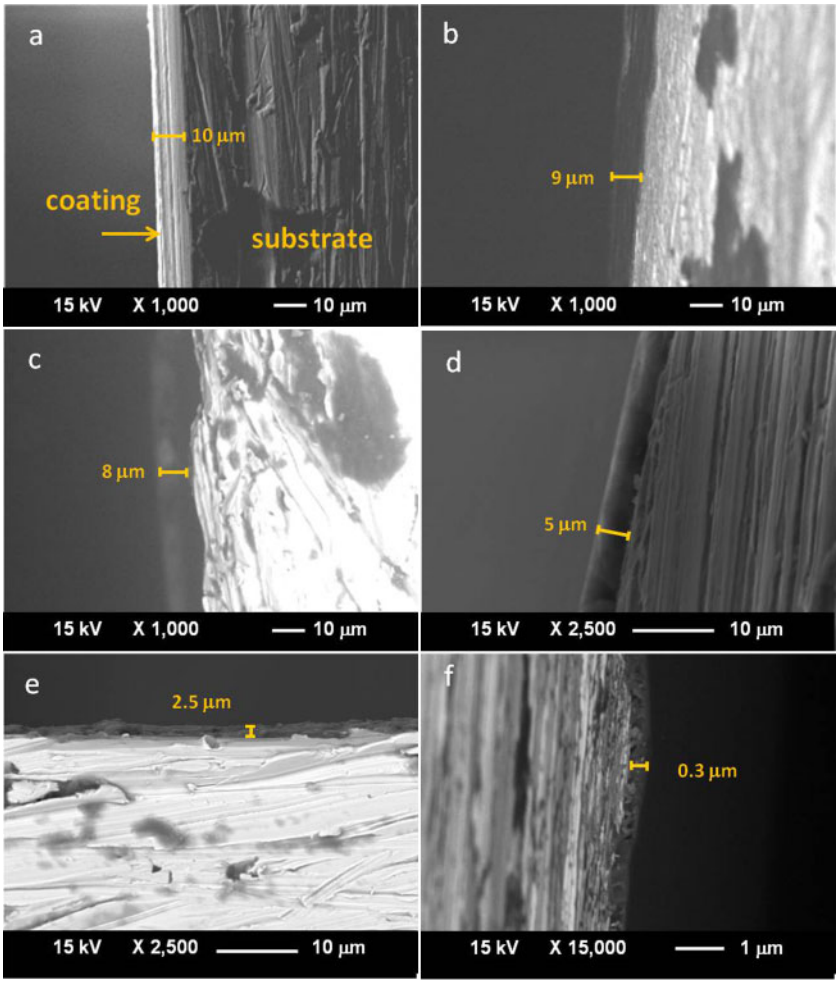

a 100–00; *b* 90–10; *c* 75–25; *d* 50–50

4 Hybrid coating micrographs transversal section

assigned to the stretching bands of the CH_2 and CH_3 groups respectively, and other vibration of group CH_3 appeared at 2974 cm^{-1}. Vibrations at 1723 and 1637 cm^{-1} corresponded to the C=O and C=C groups respectively. The bands at 1079 cm^{-1} are associated with Si–O–Si linkages, and the bands at 950 and 879 cm^{-1} corresponded to Si–OH bond; these absorption bands can be observed in all hybrid sol–gel coatings.

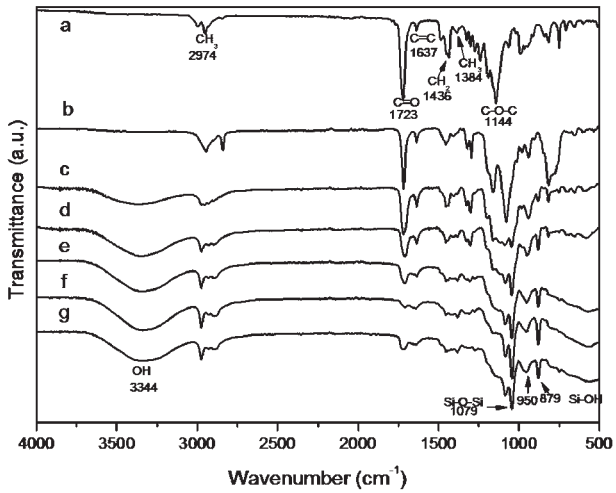

a PMMA; *b* 3-(trimethoxysilyl)propyl methacrylate; *c* 90–10; *d* 75–25; *e* 50–50; *f* 25–75; *g* 10–90

5 Fourier transform infrared spectra

Pull-off tape adhesion test (ASTM D 3359-02)

The adhesion strength of PMMA–silica hybrid coatings on stainless steel was found to be higher than for pure system PMMA coating alone, as evidenced by the smaller stripped areas (Fig. 6). The adhesion of the coating was further enhanced as the amount of TEOS component was increased in the hybrid materials. It is

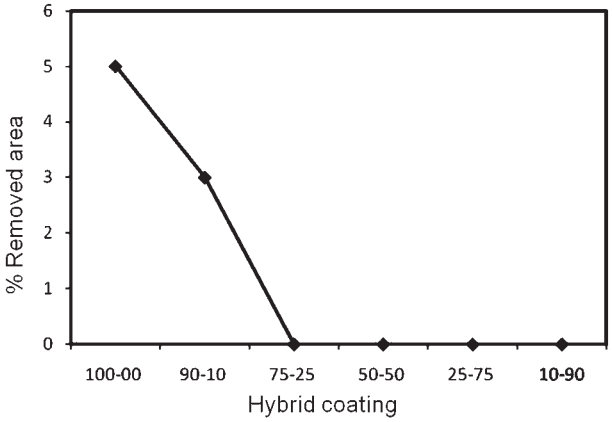

6 Measuring adhesion by tape test on PMMA–silica hybrid sol–gel coatings according to ASTM D3350

particularly noteworthy that as the TEOS was increased up to 25%, the hybrid sol–gel coating remained intact after the tape was stripped off.

Electrochemical measurements

The results obtained with 5 wt-% NaCl solution after visual evaluation analysis of the coated panels according to ASTM D610 and ASTM D714 standards, are shown in Tables 2 and 3 respectively. It is clear that the 50–50, 25–75 and 10–90 PMMA–silica hybrid coatings fail before 1500 h exposure to the 5 wt-% NaCl solution, while the 100–00 PMMA–silica hybrid coating fails after 1750 h exposure in the 5 wt-% NaCl solution, showing both blistering and rusting. On the other hand, the other systems (90–10 and 75–25 coatings) remain apparently undamaged (neither blistering nor rusting was observed on the other systems).

The behaviour of the EN resistance R_n as a function of exposure time to 5 wt-% NaCl solution for the systems studied is shown in Fig. 7. For the 100–00 PMMA–silica system, which failed on visual inspection after exposure for 1750 h, the initial R_n values were found to decrease by two orders of magnitude after only 250 h. It then increased to 500 h and declined again after 750 h, and then assumed very low values (10^5 Ω) beyond 3000 h. This behaviour is probably due to the sealing of pores by corrosion products (showing a clear tendency to decrease with time), which means that corrosion has taken place at the metal/coating interface, in good agreement with the visual evaluation previously reported. Thus, the initial barrier effect disappeared in the 100–00 PMMA–silica system, while in the other systems (90–10 and 75–25), the effect was only attenuated. With PMMA–silica coating system 90–10, the initial value of R_n decreased by one order of magnitude after 250 h, maintaining an average value of 10^6 Ω after 1750 h until the end of the test. The best performance was for the 75–25 PMMA–silica system, for which the initial R_n value decreased by half an order of magnitude after 500 h. It then increased after 1000 h and maintained an average value of 10^7 Ω until the end of the test.

Figure 7 shows that the R_n values started to fall before visible corrosion was observed (in fact, 316L stainless steel had the lowest R_n since the start the test).

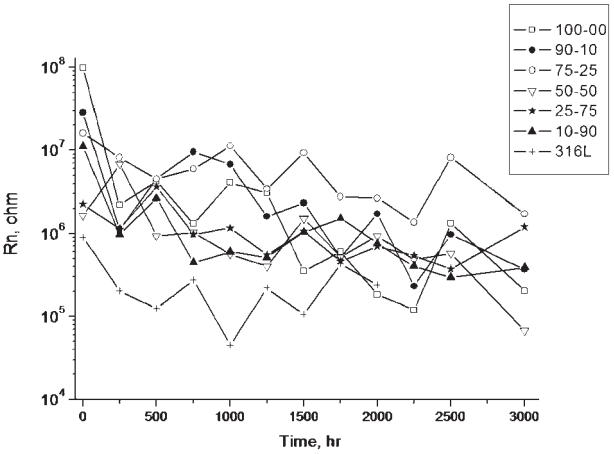

7 Noise resistance R_n as function of exposure time in 5 wt-% NaCl solution

The 75–25 coating had higher R_n values than the pure PMMA coating (100–00) during the whole immersion time, indicating the significant decrease in water uptake. This behaviour may be caused by the hydrolysis reactions of active alkoxy groups in 75–25 hybrid coating, by which the free state water absorbed can be consumed. The condensation reactions between the hydrolysed groups are also expected to improve the cross-linking of the hybrid coating. In addition, the hydrolysis products, methanol or ethanol, can also repel the permeation of water in the polymeric coatings, as reported by Flis and Kanoza.[32] The R_n behaviour of the 90–10 system can be attributed to the lower adhesion than that of the 75–25 system (*see* Fig. 6), while the R_n of the 50–50, 25–75 and 10–90 systems can be attributed to the lower barrier effect due to the reduced thickness of these coatings. It is important to mention that the preparation of thick sol–gel ceramic coatings induces the formation of cracks during the drying procedure.[33] For this reason, increasing the thickness of the coatings 25–75 and 10–90 can lead to the appearance of defects due to high ceramic content; this is confirmed by the images in Fig. 3*e* and *f*.

It is interesting to study the shape and magnitude of the current and potential noise transient signals. In Figs. 8 and 9, the potential and current time series for the 100–00 and 75–25 systems at 0 h and after exposure

Table 2 Degree of rusting (ASTM D610) after different exposure times in 5 wt-% NaCl for 316L stainless steel panels covered with PMMA–silica hybrid coatings*

Immersion time/h	100–00	90–10	75–25	50–50	25–75	10–90	316L stainless steel
0	10	10	10	10	10	10	10
500	10	10	10	10	10	10	10
750	10	10	10	10	10	10	10
1000	10	10	10	10	10	10	9
1250	10	10	10	10	9	9	8
1500	10	10	10	9	8	8	7
1750	9	10	10	8	8	7	7
2000	9	9	10	8	7		
2250	9	8	10	8	7		
2500	8	8	10	7			
3000	8	8	9	7			

*10, 9: good coatings; 8, 7: bad coatings.

Table 3 Blistering degree (ASTM D714) after different exposure times in 5 wt-% NaCl for 316L stainless steel panels covered with PMMA–silica hybrid coatings*

Immersion time/h	100–00	90–10	75–25	50–50	25–75	10–90
0	10	10	10	10	10	10
250	10	10	10	10	10	10
500	10	10	10	10	10	10
750	10	10	10	10	10	10
1000	10	10	10	10	10	10
1250	10	10	10	10	8F	8F
1500	10	10	10	8F	8F	8F
1750	8F	10	10	8F	8F	8F
2000	8F	8F	10	8M	6F	6F
2250	8M	8F	10	6F	6F	6F
2500	6F	8M	10	6F	6F	6F
2750	6M	8M	10	6F	6F	6F
3000	4M	6M	8F	6M	6F	6F

*10: good coatings; 8, 6, 4: bad coatings.

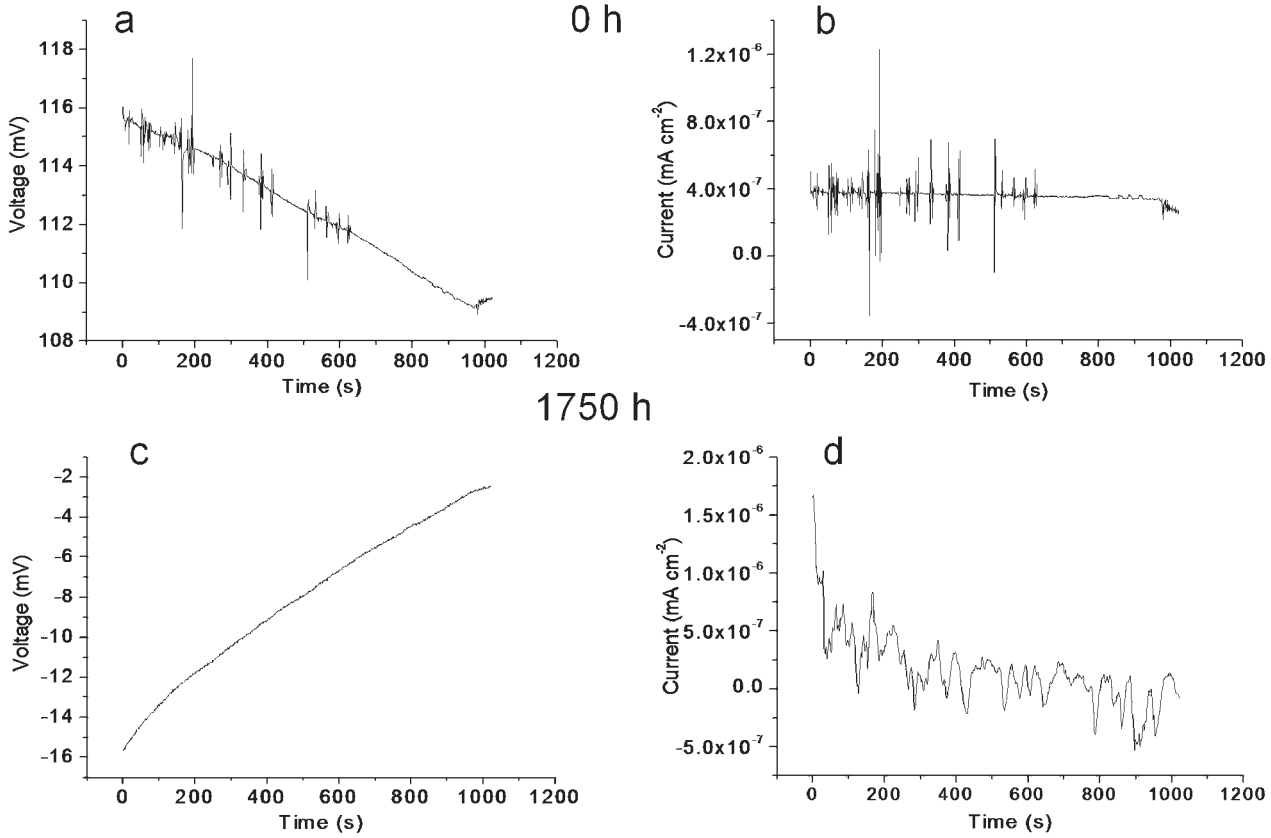

8 Time series for system 100–00 at 0 and 1750 h immersion

for 1750 h to 5 wt-% NaCl solution are shown. This exposure time was selected for comparison because the 100–00 system failed after this interval. In Fig. 8*a*, it can be seen that the potential noise values for the 100–00 system are more noble at the beginning of the exposure [109–116 mV(SCE)]. For higher times of exposure (1750 h, Fig. 8*c*), the corrosion potential decreases to more active values [between −2 and −16 mV(SCE)].

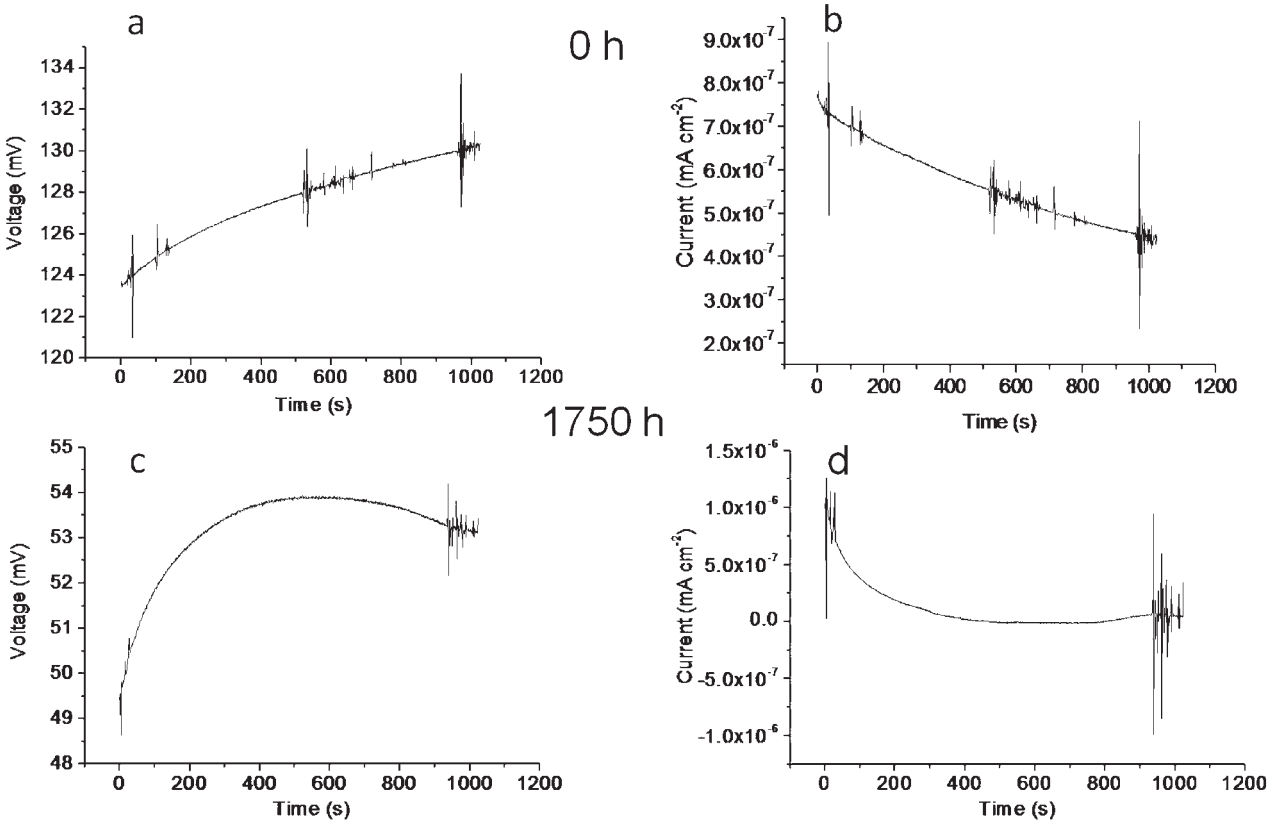

9 Time series for system 75–25 at 0 and 1750 h immersion

Note that in this figure, the longer the exposure time, (and consequently, the more degraded the coating), the lower the amplitude of the potential noise. For the 75–25 system (Fig. 9*a*), the potential noise values at the beginning [123–130 mV(SCE)] and the potential noise at 1750 h [between 49 and 54 mV(SCE)] are more noble than the 100–00 system.

For the current noise values, system 100–00 shows signals that fluctuate more when the exposure time is longer. In addition, current noise values of 4×10^{-7} mA cm^{-2} were found during the stage of protection (0 h) and between -5×10^{-7} and 1×10^{-6} mA cm^{-2} during the time of doubtful protection (1750 h), as shown in Fig. 8*b* and *d*. Whereas for the system 75–25 (Fig. 9*b*), the initial current noise values were between 4 and 8×10^{-7} mA cm^{-2}, while at 1750 h, they were between 1 and 9×10^{-7} mA cm^{-2}, showing better anticorrosive properties in good agreement with Fig. 7.

Conclusions

The present work shows that by the sol–gel method, it is possible to synthesise PMMA–silica hybrid coatings with better corrosion resistance for 316L stainless steel than that for neat polymer PMMA. The best anticorrosive properties were for the system with the ratio of 75 : 25 PMMA/silica, which has the best performance as demonstrated by visual evaluation and EN. Additionally, the excellent agreement between visual evaluation analysis and EN confirms that the latter is a useful tool for evaluating the anticorrosive performance of coatings. These results also agree with the SEM analysis, which shows that the coatings 100–00, 90–10, 75–25 and 50–50 are continuous, crack free and well bonded to the metallic substrate.

One of the potential applications for such coatings may be to protect 316L stainless steel prosthesis and decrease the release of corrosive species to neighbouring tissues as well as for aesthetic coatings of stainless steel materials.

References

1. D. A. Jones: 'Principles and prevention of corrosion', 2nd edn; 1996, Englewood Cliffs, NJ, Prentice-Hall.
2. D. C. Hansen: *Electrochem. Soc. Interface*, 2008, **17**, (2), 31–34.
3. L. L. Shreir, R. A. Jarman and G. T. Burstein (eds.): 'Corrosion', 3rd edn; 1994, Oxford, Butterworth-Heinemann.
4. D. A. López, N. C. Rosero-Navarro, J. Ballarre, A. Durán, M. Aparicio and S. Ceré: *Surf. Coat. Technol.*, 2008, **202**, 2194–2201.
5. H. S. Klapper and J. Goellner: *Corros. Sci.*, 2009, **51**, 144–150.
6. J. Ballarre, D. A. López, N. C. Rosero, A. Durán, M. Aparicio and S. M. Ceré: *Surf. Coat. Technol.*, 2008, **203**, 80–86.
7. C. Martinez, M. Sancy, J. H. Zagal, F. M. Rabagliati, B. Tribollet, H. Torres, J. Pavez, A. Monsalve and M. A. Paez: *J. Solid State Electrochem.*, 2008, **13**, 1327–1337.
8. C. X. Li and T. Bell: *Corros. Sci.*, 2006, **48**, 2036–2049.
9. 'Standard practice for surface preparation and marking of metallic surgical implants', ASTM F-8604, ASTM International, West Conshohocken, PA, USA, 2004.
10. 'Standard specification for chemical passivation treatments for stainless steel parts', ASTM A967-01, ASTM International, West Conshohocken, PA, USA, 2001.
11. K. Rose, S. Dzyadevych, R. Fernández-Lafuente, N. Jaffrezic, G. Kuncova, V. Mate and P. Scully: *J. Coat. Technol. Res.*, 2008, **5**, 491–496.
12. T. Sasaki and K. Kamitani: *J. Sol–Gel Sci. Technol.*, 2008, **46**, 180–189.
13. M. L. Zheludkevich, I. Miranda Salvado and M. G. S. Ferreira: *J. Mater. Chem.*, 2005, **15**, 5099–5111.
14. T. P. Chou, C. Chandrasekaran, S. J. Limmer, C. Nguyen and G. Z. Cao: *J. Mater. Sci. Lett.*, 2002, **21**, 251–255.
15. J. M. Yeh, C. J. Weng, W. J. Liao and Y. W. Mau: *Surf. Coat. Technol.*, 2006, **201**, 1788–1795.
16. S. Ono, H. Tsuge, Y. Nishi and S. Hirano: *J. Sol–Gel Sci. Technol.*, 2004, **29**, 147–153.
17. J. Gallardo and P. Galliano: *J. Sol–Gel Sci. Technol.*, 2001, **21**, 65–74.
18. M. Zaharescu, L. Predoana, A. Barau, D. Raps, F. Gammel, N. C. Rosero-Navarro, Y. Castro, A. Durán and M. Aparicio: *Corros. Sci.*, 2009, **51**, 1998–2005.
19. D. Raps, T. Hack, J. Wehr, M. L. Zheludkevich, A. C. Bastos, M. G. S. Ferreira and O. Nuyken: *Corros. Sci.*, 2009, **51**, 1012–1021.
20. M. Behzadnasaba, S. M. Mirabedinia, K. Kabiria and S. Jamalib: *Corros. Sci.*, 2011, **53**, 89–98.
21. N. C. Rosero-Navarro, S. A. Pellice, A. Durán and M. Aparicio: *Corros. Sci.*, 2008, **50**, 1283–1291.
22. Y. Zhang, H. Ye, H. Liu and K. Han: *Corros. Sci.*, 2011, **53**, 1694–1699.
23. N. P. Tavandashti, S. Sanjabi and T. Shahrabi: *Prog. Org. Coat.*, 2009, **65**, 182–186.
24. T. P. Chou, C. Chandrasekaran, S. J. Limmer, S. Seraji, Y. Wu, M. J. Forbess, C. Nguyen and G. Z. Cao: *J. Non-Cryst. Solids*, 2001, **290**, 153–162.
25. F. Mammeri, L. Rozes and C. Sanchez: *J. Sol–Gel Sci. Technol.*, 2003, **26**, 413–417.
26. D. J. Mills and S. Mabbutt: *Prog. Org. Coat.*, 2000, **39**, 41–48.
27. R. L. De Rosa, D. A. Earl and G. P. Bierwagen: *Corros. Sci.*, 2002, **44**, 1607–1620.
28. S. Mabbutt, D. J. Mill and C. P. Woodcock: *Prog. Org. Coat.*, 2007, **59**, 192–196.
29. K. Hladky and J. L. Dawson: *Corros. Sci.*, 1981, **21**, 317–322.
30. K. Hladky and J. L. Dawson: *Corros. Sci.*, 1982, **22**, 231–237.
31. R. Cottis and S. Turgoose: 'Electrochemical Impedance and noise', in 'Corrosion testing made easy series', (ed. B. C. Syrett), 68; 1999, Houston, TX, NACE International.
32. J. Flis and M. Kanoza: *Electrochim. Acta*, 2006, **51**, 2338–2345.
33. M. Gluglielmi: *J. Sol–Gel Sci. Technol.*, 1997, **8**, 443–449.